

Short Communication

Mechanism for the Formation of Cuprous Oxide Nanowires in AAO template by Electrodeposition

Babar Shazad Khan², Adnan Saeed², Sardar Sikandar Hayat³, Aiman Mukhtar¹, Tahir Mehmood^{1,*}

¹ The state key laboratory of Refractories and Metallurgy, Hubei Collaborative Innovation Center for Advanced Steels, International Research Institute for Steel Technology, Wuhan University of Science and Technology, Wuhan, P. R. China

² Department of Physics, Government College Women University, 51310, Sialkot, Pakistan

³ Department of Physics, Hazara University, 21300, Mansehra, Pakistan

*E-mail: tahir10621@yahoo.com

Received: 25 September 2016 / Accepted: 16 December 2016 / Published: 30 December 2016

The effect of potential and pH on the formation of Cu₂O and Cu nanowires in AAO template have systematically been studied by Potentiostate, XRD, SEM, TEM and EDX. The pure Cu₂O nanowires were electrodeposited at voltage (−0.3 V) and pH (8.2). At higher voltage (−0.6 V and −0.5 V) with low pH 8.2, there was co-existence of Cu and Cu₂O nanowires. At voltage −0.5 V with pH 9, the pure Cu₂O nanowires are formed. A mechanism is proposed for the formation of cuprous oxides nanowires. The formation of pure Cu₂O nanowires can be attributed to the formation of large size critical Cu nuclei, the larger size of nuclei favors the formation of pure cuprous oxides nanowires.

Keywords: Electrochemical Deposition; Cuprous Oxide; Growth; Nanowires

1. INTRODUCTION

Cuprous oxide (Cu₂O) is an attractive p-type semiconductor with energy band gap of 2.0-2.2 eV [1]. The high optical absorption coefficient in the visible range and noble electrical properties of Cu₂O make it an attractive semiconductor [2]. Daltin et al. fabricated cuprous oxide films and nanowires in a polycarbonate membrane by cathodic reduction of an alkaline cupric lactate solution [3]. Lee et al fabricated Cu/Cu₂O composite nanowires on Si via anodic alumina oxide (AAO) template by electrodeposition at different current densities [4]. At low current density pure Cu₂O films are formed, but at higher current density pure Cu nanostructured is obtained. Deposition from intermediate current density Cu/Cu₂O composite is formed. According to their view, Cu and Cu₂O can be formed by altering the H⁺ and OH[−] ions due to variation of current density. Wang et al explained the mechanism of formation of Cu, Cu/Cu₂O and pure Cu₂O in AAO template. They explained that the evolution of

hydrogen may responsible for the formation of pure Cu_2O . At lower pH there is a lot of H^+ ions present in the pores to form the oxide nanowires, but at high pH the hydrogen evolution depleted and concentration of OH^- ions increased to react with Cu^+ ions to form the Cu_2O .

In their study they only relate the cuprous oxide formation with the hydrogen evolution. We believe that besides with the hydrogen evolution the most important factor is the size of critical nuclei. Moreover, the elemental processes of electrodeposition are still not well understood. Therefore, we first give the results on effect of pH, and deposition potential on the formation of Cu_2O and Cu nanowires in AAO template and then proposed a mechanism to justify the effect of different experimental conditions on the formation of Cu_2O and Cu nanowires.

2. EXPERIMENTAL DETAILS

The porous anodic alumina oxide (AAO) templates were prepared via a two-step anodization procedure, like in our previous work [5-10]. The templates obtained by this method have hexagonally arranged cylindrical pores of about 50 nm diameter and the length of about 65 μm . In order to deposit metal oxide nanowires into the pores of AAO templates, a gold film was sputtered onto the back side of the AAO templates to serve as a working electrode with area of 0.608 cm^2 ($= 0.25\pi(0.88\text{cm})^2$).

The potentiostatic deposition was performed in a three electrodes cell. The electrolytes was a mixture of CuSO_4 (0.356 M) and H_3BO_3 (0.68 M) solutions. After adding certain amount of NaOH, the electrolyte was stirred for the whole night by a magnetic stirrer and then pH value was adjusted to 8.2, and 9 with 1 M NaOH/ H_2SO_4 . A graphite electrode with area 14.7 cm^2 ($= 4.2\text{cm} \times 3.5\text{cm}$) was used as counter electrode and a Saturated Calomel Electrode (SCE) as reference electrode. Direct-current electrodeposition was conducted at three different voltages (-0.3 V, -0.5 V, and -0.6 V) for pH 8.2, and at -0.5 V for pH 9.

The structural analysis of electrodeposited nanowires was done by X-ray Diffraction (XRD, Y-2000) with Cu-K_α radiations. The electrodeposited nanowires were analyzed by scanning electron microscope (SEM, JEOL JSM-6700F), and TEM (TEM, FEI Tecnai G² 20 UTwin) with energy dispersive spectrometer (EDS, Model: Le350 PentaFETx-3). For SEM observation, AAO templates were partly dissolved in 5 wt.% NaOH solution and carefully washed many times. Templates were fully dissolved in 5 wt.% NaOH solution and subsequent rinsing with distilled water for TEM observation.

3. RESULTS

Figure 1a shows the XRD patterns of Cu/ Cu_2O nanowires deposited in the solution of pH 8.2 at different potentials of -0.3 V, -0.5 V, and -0.6 V at room temperature. The XRD patterns were collected from the top side of nanowires. It was found that the electrodeposition of copper oxide nanowires lie on the deposition potentials.

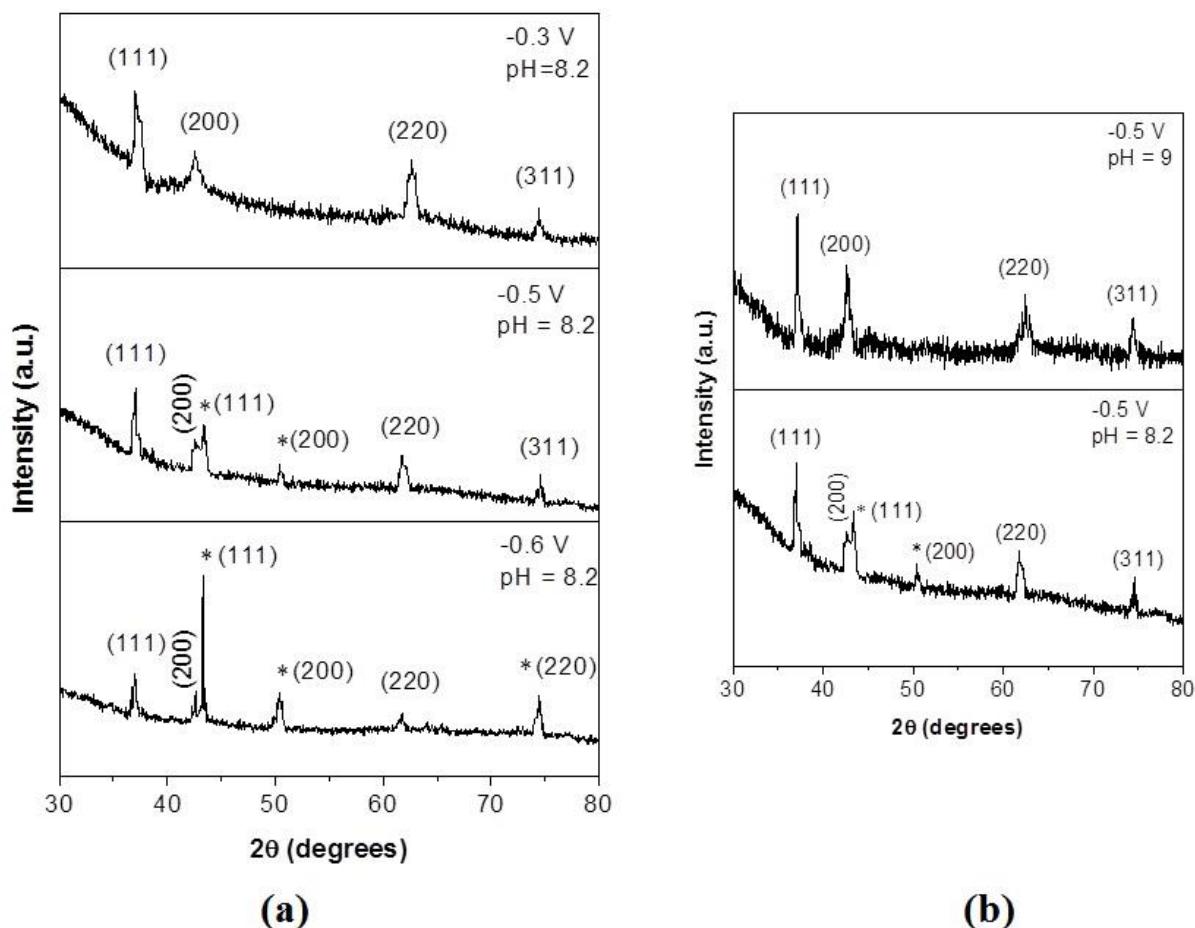


Figure 1. XRD patterns of Cu/Cu₂O nanowires deposited into the nanopores of AAO templates: (a) at -0.3 V, -0.5 V, and -0.6 V with pH 8.2, and (b) at -0.5 V with pH 8.2 and 9.0.

When electrodeposition is performed in the same electrolytic cell at different potentials, the Cu nanowires transformed to copper oxides. At -0.6 V, there was a mixture of Cu/Cu₂O nanowires. Cu nanowires grows along (111), (200), and (220) planes. On the other hand, Cu₂O nanowires also grow along (111), (200), and (220) plane. The intensity of the peaks for the Cu nanowires decreases with the decrease in potential, while for Cu₂O nanowires it increases. When the deposition potential is decreased to -0.5 V, the Cu-(220) plane vanished and a new plane for Cu₂O-(311) was observed. Decreasing the potential to -0.3 V, all the peaks for Cu nanowires were vanished and only the pure Cu₂O nanowires phases were existed in the XRD pattern.

To study the effect of pH on the electrodeposition of Cu₂O nanowires, Cu/Cu₂O nanowires were deposited at room temperature with -0.5 V and different pH . Figure 1b shows the XRD patterns of Cu/Cu₂O nanowires deposited with pH of 8.2 and 9.0. At lower value of pH there was a mixture of Cu/Cu₂O nanowires, by increasing the pH value to 9.0, all the phases formed in the XRD pattern shows the pure Cu₂O nanowires. The phenomenon for the electrodeposition of pure Cu₂O nanowires will be discussed in the next section.

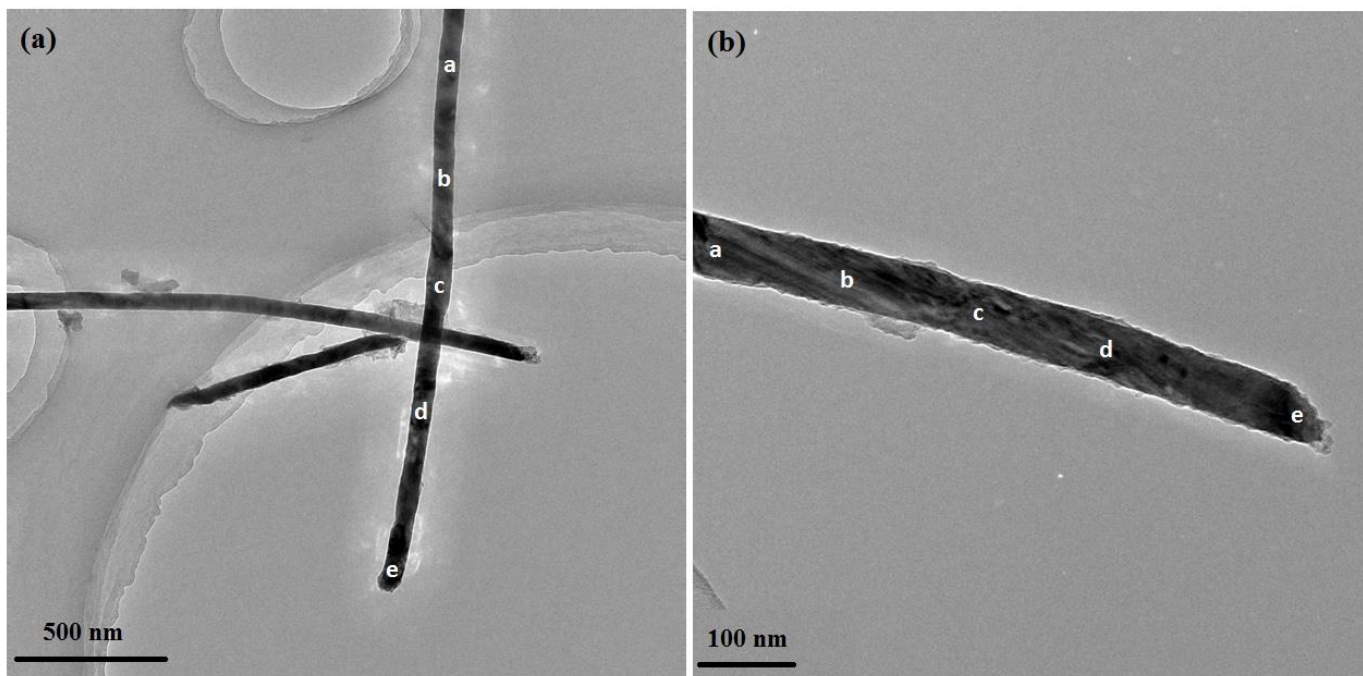


Figure 2. SEM images: (a) -0.3 V and pH 8.2, and (b) pH 9.0 at -0.5 V.

Figure 2 shows the TEM image of electrodeposited Cu_2O nanowires. The chemical composition for the Cu/Cu_2O nanowires is shown in Table 1.

Table 1. Chemical composition for the Cu/Cu_2O nanowires

Points	pH 8.2, V = -0.3 V		pH 9, V = -0.5 V	
	Cu (at. %)	O (at. %)	Cu (at. %)	O (at. %)
a	87.88	12.12	88.84	11.56
b	87.73	12.27	88.60	11.40
c	87.81	12.19	88.33	11.67
d	87.48	12.52	88.04	11.96
e	87.95	12.05	88.71	11.29

To get the better understanding for chemical composition, a single electrodeposited nanowire at -0.3 V with pH 8.2 was selected and at different points (a, b, c, and d) spectrum was measured, as shown in Fig. 3a. The spectrums show that at all different points the Cu/O ratio ($\sim 88\%$ of Cu and $\sim 12\%$ of O) is same, which means that the whole nanowire is of pure Cu_2O . Figure 3b shows the TEM image of a single Cu_2O nanowire deposited at -0.5 V with pH 9.0. The chemical composition of Cu and O is $\sim 86\%$ and $\sim 14\%$, respectively, indicating that at high pH with high potential, pure Cu_2O nanowires can be grown.

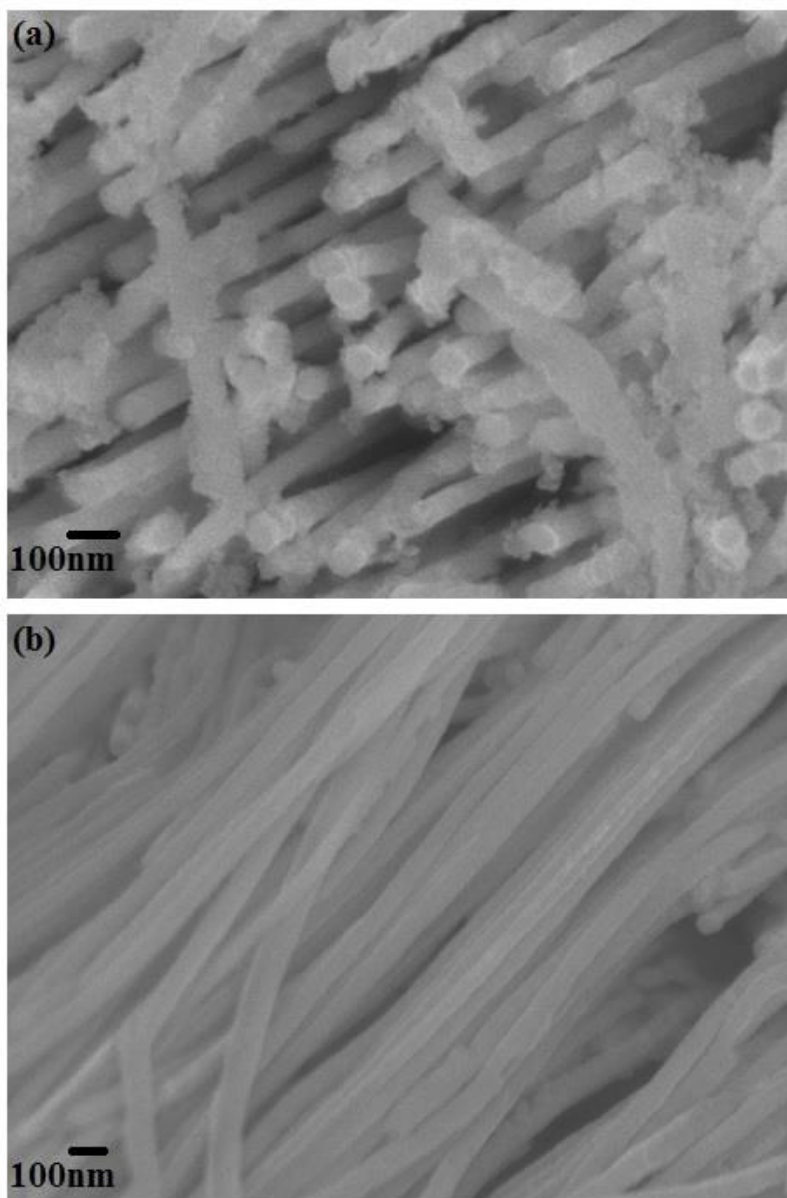


Figure 3. TEM image of electrodeposited Cu_2O nanowires: (a) at -0.3 V with pH 8.2, and (b) at -0.5 V with pH 9.0.

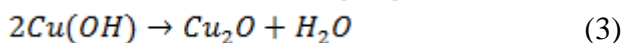
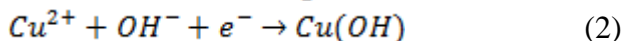
Figure 3a illustrates the SEM image of Cu_2O nanowires deposited at -0.3 V and pH 8.2, and Fig. 3b shows the image with pH 9.0 at -0.5 V. The diameter of the Co nanowires is the same as that of the pores of AAO template ($\sim 50\text{nm}$), which means that the hexagonal pores of AAO templates are fully filled.

4. DISCUSSION

The formation of Cu nanowires is attributed to the charge transfer reactions represented in the following equations[11]



In alkaline electrolytes the higher pH favors the formation of Cu_2O [12], the Cu^{+} ions react with OH^{-} ions to form the Cu_2O nanowires; the possible reactions are given by:



The formation of copper oxides takes place on a polycrystalline Au surface. The geometrically irregular surface structure of the polycrystalline Au in nanoscale leads the formation of clusters with various shapes. is not smooth but geometrically irregular in the nanoscale. This leads to the clusters formed on the Au surface having various shapes. The formation of Cu_2O nanowires in the pores of AAO template is connected with pH and the applied potential. Figure 4 shows the mechanism of forming Cu_2O at different potentials and pH , and is described below.

First Cu_2O nuclei with different sizes were formed depending on the bath conditions. Then, these nuclei undergo crystallization process and grow as Cu_2O nanowires inside the pores of AAO template. Many researchers confirmed that a local increase of the pH at the pore base region of the AAO template is required for the formation of Cu_2O in the acidic electrolyte [13]. The formation of copper oxides takes place when Cu^{+} ions react with OH^{-} ions. At lower $pH < 8$ the reduction process is thermodynamically favored and copper metal forms [12] as expressed in Eq. (1). The higher $pH > 8$ favors the formation of Cu_2O [14, 15], because high pH is likely response to increase in the concentration of hydroxyl ions in the solution. By neglecting the complexity of the relevant reaction, these OH^{-} ions react with the Cu^{+} ions to form copper hydroxide nuclei according to Eq. (2). Further, these formed copper hydroxide nuclei dehydrate in the pores of AAO and form Cu_2O nanowires by reaction mentioned in Eq. (3).

In crystal growth, the surface morphology is largely determined by the crystal surface with the slowest growth rate. The deposition rate of copper oxide perpendicular to the surface is proportional to the voltage and can be expressed as:

$$R = MV/z\rho F \quad (4)$$

where M is the molar mass of Cu_2O (143.1g/mol^{-1}), V is the applied potential, $z=2$ is the number of electrons participating in the electrodeposition of one molecule of Cu_2O , ρ is the bulk density of Cu_2O (5.9 g.cm^{-3}) and F is the Faraday constant (96487 C. mol^{-1}). The growth rate is directly related to the voltage, so lower the voltage is, lower will be the deposition. This rate can be argued by using the classical electrochemical nucleation theory, the free energy of formation of a 3 dimension cluster N , $\Delta G(N)$, is given by [16, 17]

$$\Delta G(N) = -Nze\eta + bN^{\frac{2}{3}} \quad (5)$$

where z is the valence of the metal ions, e is the elementary electric charge, η is the overpotential ($\eta = V - V_{eq}$, where V is the applied potential and V_{eq} the equilibrium potential), b is the constant depending on the geometrical shape of the cluster. Taking the derivative of Eq. (1) with respect to N and equating to zero yields the size of the critical cluster, N_c

$$N_c = \left(\frac{2b}{3ze\eta} \right)^3 \quad (6)$$

From eq. (2), it can be seen that the size of the critical cluster N_c depends on both overpotential (η) and the geometrical shape of the cluster (b). The size of the critical cluster decreases with increasing the overpotential.

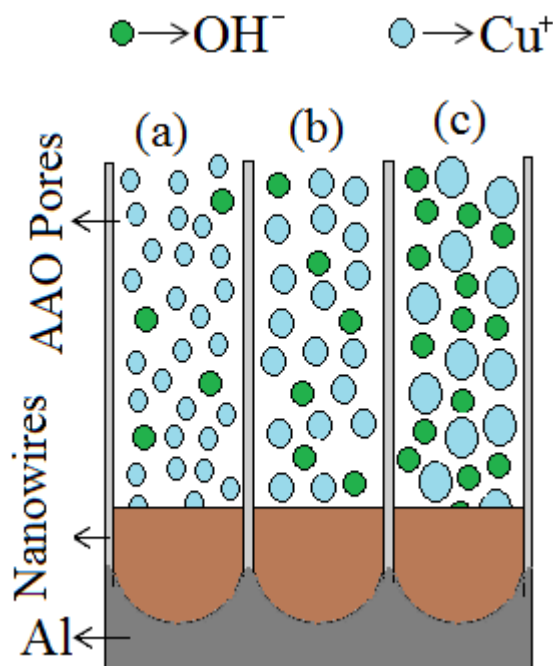


Figure 4. Schematic illustration showing the formation of Cu_2O nanowires in pores of AAO template: (a) Low voltage and low pH , forming small Cu^+ nuclei and less OH^- ions, (b) Less high voltage and Low pH , and (c) low voltage and high pH . (Not drawn in scale).

The physical meaning of the critical cluster is that the critical cluster can be either transformed into a crystal nucleus for growth if gaining one atom or dissolved if losing one atom [17]. It can therefore be seen from eq. (2) that the sizes of the critical clusters N_c formed under a fixed deposition potential should have a distribution because of different shape factors (b). When the potential is high (-0.6 V) the sizes of critical clusters become small, these small can find much space in the pores to reach the surface and to adsorbed to form Cu nanowires. As the potential become less negative the size distribution of critical clusters shifts to large size, larger sizes react with the present OH^- ions and dehydrate to form Cu_2O , but still some of Cu nuclei were there to adsorb as the Cu nanowires. For deposition at -0.3 V the size is large enough that all coming nuclei could react with OH^- ions to deposit the pure Cu_2O nanowires.

5. CONCLUSIONS

It is concluded that the formation of pure Cu_2O nanowires at (-0.3 V) with pH (8.2) and at (-0.5 V) with pH (9.0) in pores of AAO templates can be accredited to larger Cu critical clusters. At a fixed potential, there is a distribution in size of the critical clusters, which can be shifted to large sizes at low

potential. The sizes of all critical clusters at -0.6 V can be small enough, find much space in the pores to adsorb and to form Cu nanowires. At -3.0 V, all Cu critical clusters can be large in size enough, decreasing the number of Cu nuclei in the pore base region to react with the existing OH^- ions, favoring the growth of Cu_2O nanowires.

ACKNOWLEDGMENT

This work was supported by Higher Education Commission, Pakistan, Grant numbers SRGP-868 and SRGP-869. The authors are thankful to Wuhan University of Science and Technology, Wuhan, China for providing the lab facilities.

References

1. I. Grozdanov, *Mater. Lett.*, 19 (1994) 281.
2. A.O. Musa, T. Akomolafe, M.J. Carter, *Sol. Energy Mater. Sol. Cells*, 51 (1998) 305.
3. A.L. Daltina, A. Addadb, J.P. Chopart, *J. Cryst. Growth*, 282 (2005) 414.
4. Y.H. Lee, I.C. Leub, M.T. Wu, J.H. Yen, K.Z. Fung, *J. Alloys Compd.*, 427 (2007) 213.
5. H. Masuda, K. Fukuda, *Science*, 268 (1995) 1466.
6. M. Tan, X. Chen, *J. Electrochem. Soc.*, 159 (2012) K15.
7. T. Mehmood, B. Shahzad Khan, A. Mukhtar, X. Chen, P. Yi, M. Tan, *Mater. Lett.*, 130 (2014) 256.
8. B. Shahzad Khan, T. Mehmood, A. Mukhtar, M. Tan, *Mater. Lett.*, 137 (2014) 13.
9. Tahir Mehmood, Aiman Mukhtar, Honghong Wang, B.S. Khan, *International Journal of Materials Research*, 106 (2015) 1.
10. B.S. Khan, A. Mukhtar, T. Mehmood, M. Tan, *Journal of Nanoscience and Nanotechnology*, 16 (2016) 1.
11. S. Leopold, M. Herranen, J.-O. Carlsson *J. Electrochem. Soc.*, 148 (2001) C513.
12. B. Beverskog, I. Puigdomenech, *J. Electrochem. Soc.*, 144 (1997) 3476.
13. X. Wang, C. Li, G. Chen, L. He, H. Cao, B. Zhang, *Solid State Sciences*, 13 (2011) 280.
14. L. Wang, N. De Tacconi, C. Chenthamarakshan, K. Rajeshwar, M. Tao, *Thin Solid Films*, 515 (2007) 3090.
15. B. Beverskog, I. Puigdomenech, *J. Electrochem. Soc.*, 144 (1997) 3476.
16. V.A. Isaev, O.V. Grishenkova, *Electrochem. Commun.*, 3 (2001) 500.
17. M. Paunovic, M. Schlesinger, *Fundamentals of Electrochemical Deposition*, Wiley, New York, (1998).

© 2017 The Authors. Published by ESG (www.electrochemsci.org). This article is an open access article distributed under the terms and conditions of the Creative Commons Attribution license (<http://creativecommons.org/licenses/by/4.0/>).